The "Other" Fibonacci Spiral and Binet Spirals

Cye H. Waldman

cye@att.net

Introduction

In a previous paper (Waldman: 2013) we described the classical Fibonacci spiral, which is composed of quarter-circular arcs that grow as the Fibonacci sequence. This is a pseudospiral, in the sense that the curvature does not grow monotonically. It is based solely on the Fibonacci sequence and there are no other mathematical functions involved.

In the present paper we seek another type of Fibonacci spiral, one based on Binet's formula for the Fibonacci sequence, and which can be analytically continued into the entire complex plane. It would be surprising if this had never been done before, and indeed it has. We were seeking a *new* class of spirals from the Binet formula, but alas, the best laid schemes…

In this paper we will explore the Fibonacci spirals that accrue from the Binet formula, along with its derivatives and fractional derivatives, both real and complex. We will show that comparable results are found with the Binet functions for the generalized Fibonacci and Lucas sequences. The defining quality of these spirals is that they occur for negative values of the argument and the *x*-axis crossings are equal to the (negative) sequence. Self-similarity of the spirals will also be discussed.

Drawing from the literature, we will describe the three-dimensional curve and surface that arise from the (original) Binet formula and extend this work into the generalized Binet formulae.

Finally, we will have some disparaging remarks about an erroneous take on the Fibonacci numbers in the complex plane.

Binet's formula

Every sequence defined by a linear recurrence with constant coefficients has a closed-form solution. That for the Fibonacci numbers has become known as Binet's formula, even though it was known to de Moivre about a century earlier. Without any further ado,

$$F(n) = \frac{\varphi^n - \psi^n}{\varphi - \psi} \tag{1}$$

where φ is the golden ratio and ψ is variously called the conjugate (root) of φ or its complement, i.e., $\varphi + \psi = 1$. We prefer complement since everything going forward will be in complex variables.

We can analytically continue Eq. (1) into the complex plane by merely replacing the discrete variable *n* by the variable $z = x + i\,y;\ x, y \in \mathbb{R}$. However, the present effort will focus on the case of real variables, i.e., $z = x$, although the resulting function will be complex. Thus we may write

$$F(z)=\frac{\varphi^{x}-\psi^{x}}{\varphi-\psi} \tag{2}$$

where we write $F(z)$ as a reminder that the F is complex. In a similar way we can develop the analytical continuation of the Lucas numbers

$$L(z)=\frac{\varphi^{x}+\psi^{x}}{\varphi+\psi}=\varphi^{x}+\psi^{x} \tag{3}$$

where φ and ψ are as above and the denominator is unity since they are complementary, as noted previously. We will return to the Lucas numbers later. For now, let it suffice to say that everything we say about $F(z)$ applies to $L(z)$ as well.

We began this effort with the thought that we could develop a *family* of Fibonacci spirals beyond the classical form. However, as we shall see, Eq. (2) and all its derivatives lead to essentially a single spiral, hence, the "other" Fibonacci spiral. Well, not exactly. But we will show that Eq. (2) and all its derivatives are self-similar for all regular and fractional (including complex) derivatives for sufficiently large (negative) x.

Let us begin with a plot of Eq. (2) over the full range of x, by which we mean a plot of the imaginary part of $F(z)$ versus the real part. Figure 1 shows the results. The negative (left) and positive (right) values of x are shown separately for clarity (since they differ greatly in scale). The red asterisks indicate the Fibonacci sequence for negative and positive numbers as appropriate. Notice the loop on the positive side due to the repeating unity in the sequence. The full sequence shown is $F(n)=\{-55,34,-21,13,-8,5,-3,2,-1,1,0,1,1,2,3,5,8,13,21,34,55\}$. The defining feature of these curves is that every real-axis crossing is a Fibonacci number.

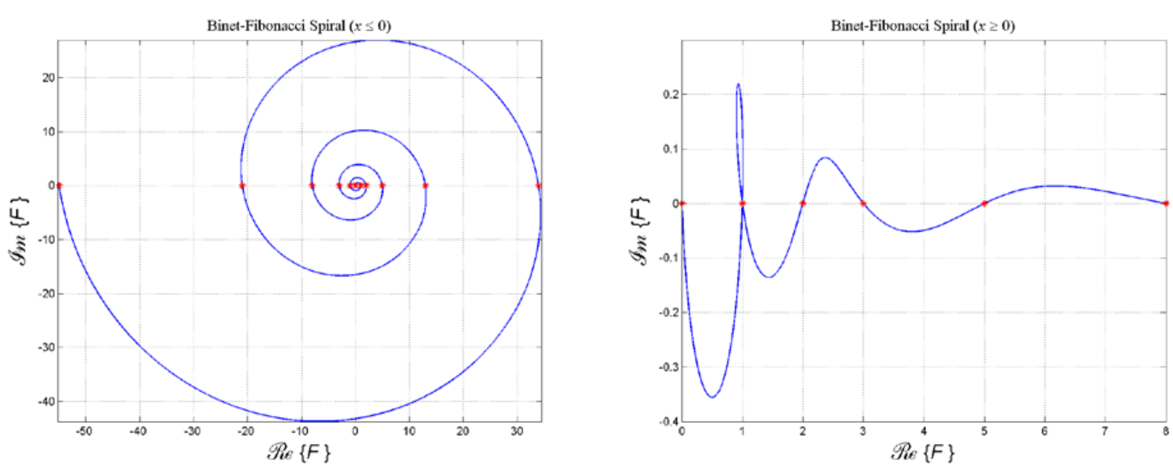

Figure 1: The Binet-Fibonacci spirals for negative and positive values of *x*.

Similar figures have appeared in the literature and we make no claim of originality [see, for example, de Bruijn (1974) and Knott (1)].

Now consider the derivatives of $F(z)$. These may be expressed as follows,

$$D^q F(z) = \frac{d^q F(z)}{dz^q} = \frac{(\ln\varphi)^q \varphi^x - (\ln\psi)^q \psi^x}{\varphi - \psi} \tag{4}$$

where we use the fractional calculus nomenclature and fractional order q as a reminder that anything goes. Parenthetically, there is no consensus in the literature as to the fractional derivative of the exponential. We take it that the α-th derivative of $e^{\lambda x}$ is equal to $\lambda^\alpha e^{\lambda x}$.

The argument for self-similarity is quite straightforward. For $x \in \mathbb{R}^-$ and $x \lesssim -3$, the second term dominates and we have

$$D^q F(z) \approx -\frac{(\ln\psi)^q \psi^x}{\varphi - \psi} = -\frac{(\ln\psi)^q e^{x\ln\psi}}{\varphi - \psi} \tag{5}$$

Thus, we see that the function and its derivatives reduce to single logarithmic spiral, excepting that they differ in magnitude and rotation for any real or complex q. In other words, they are self-similar. For example, for integer values of q, the magnitude increases by $|\ln\psi| \approx 3.178$ and is rotated by $\operatorname{Arg}(\ln\psi) \approx 1.723$ (or ~98.71°) for each unit increase in n.

Figure 2 shows a plot of $F(z)$ and its first twenty (integer) derivatives for $x \in [-10,0]$. The curves were scaled and rotated to conform to $F(z)$. The panel on the left shows the complete curve, while that on right shows a ten-fold zoom to show the details for small n, where self-similarity breaks down. Figure 3 shows a similar plot, except that we used twenty random complex values of $q \in (0-0i, 10-10i)$. The results are predictably similar to Figure 2.

A cursory look indicates the differintegration, e.g., $\operatorname{Re}\{q\} < 0$, will also give similar results. But the extent to which this can be pushed has not been fully explored. Figure 4 shows similar results for twenty "integrations" for orders $-3.5 < \operatorname{Re}\{q\} < 0$. Obviously, the general rule of self-similarity holds for large n, but perhaps the concept of "large" has to be modified. Notice also that in all the differintegration with complex q we have confined ourselves to negative imaginary parts. This is because the scaling distorts the relative importance of the φ-term in Eq. (4). If we used Eq. (5) everything would be copacetic.

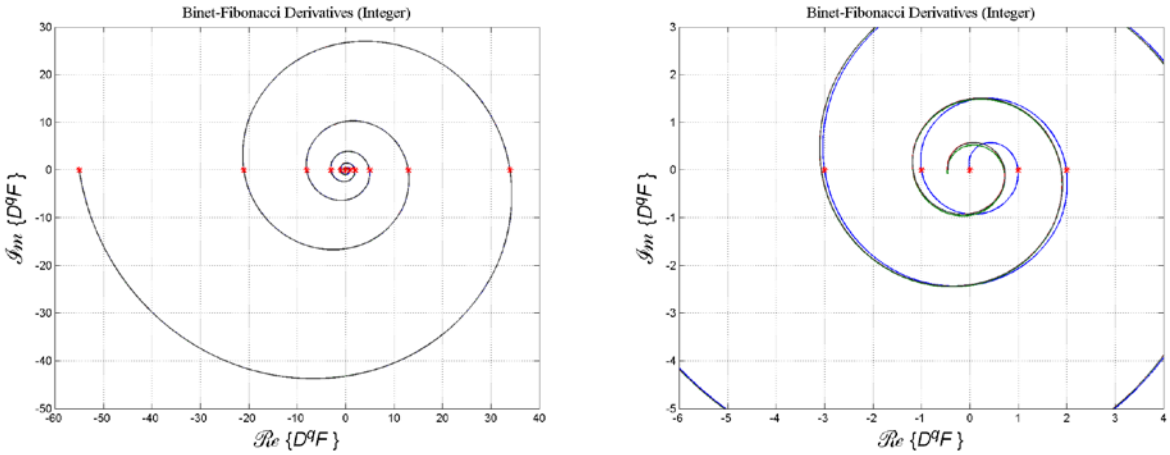

Figure 2: Binet-Fibonacci and consecutive integer derivatives.

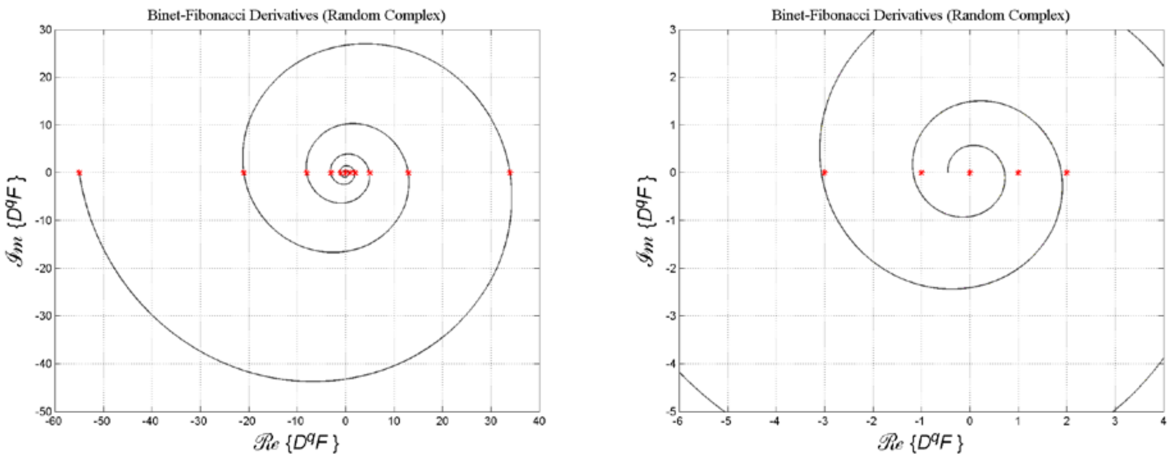

Figure 3: Binet-Fibonacci and random complex derivatives.

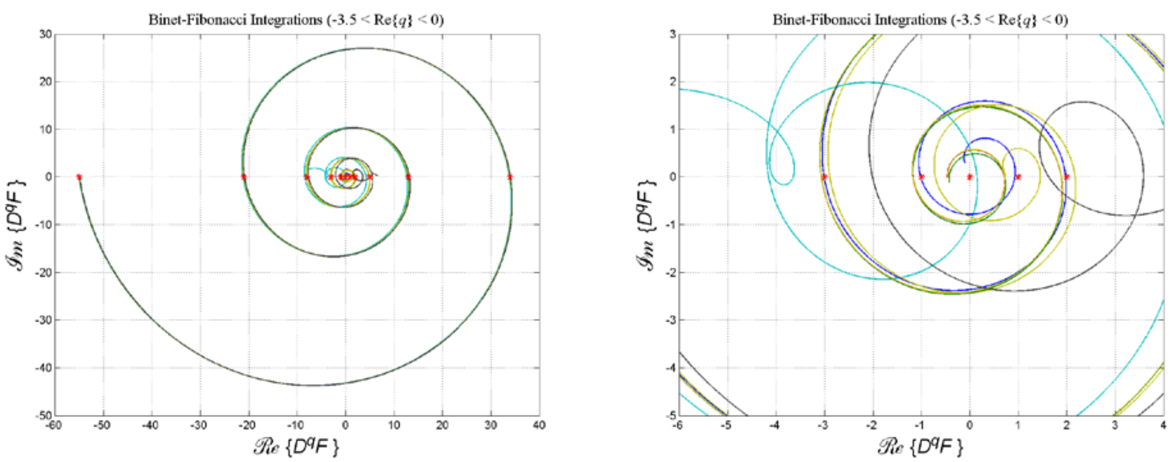

Figure 4: Binet-Fibonacci and random complex integrations.

Generalization of the Binet formulae

Many authors have successfully extended the Binet formula to variations of the Fibonacci sequence as well as other sequences. For example, Maynard (2008) derives an expression for the following sequence

$$f_0 = 0, \quad f_1 = 1, \quad f_n = a\, f_{n-1} + b\, f_{n-2} \quad \text{for } n \geq 2 \tag{6}$$

Then, for $a, b \in \mathbb{R}^+$

$$\begin{gathered} f_n = \frac{\alpha^n - \beta^n}{\alpha - \beta} \\ \alpha, \beta = \left(a \pm \sqrt{a^2 + 4b}\right) \Big/ 2 \end{gathered} \tag{7}$$

This is in agreement with Eq. (2) for $a = b = 1$, which is the Fibonacci sequence.

The Lucas numbers, i.e.,

$$f_0 = 2, \quad f_1 = 1, \quad f_n = f_{n-1} + f_{n-2} \quad \text{for } n \geq 2 \tag{8}$$

also have a well-known Binet solution that is given by

$$L_n = \varphi^n + \psi^n = \varphi^n + \left(-1/\varphi\right)^n \tag{9}$$

where φ and ψ are as given in Eq. (1). We consider generalized Lucas numbers given by

$$f_0 = 2, \quad f_1 = a, \quad f_n = a\, f_{n-1} + b\, f_{n-2} \quad \text{for } n \geq 2 \tag{10}$$

Following Maynard's analysis, we found that

$$f_n = \alpha^n + \beta^n \tag{11}$$

where α and β are as given in Eq. (7). We do not know if this is an original result because there is a rather large body of literature on generalized Binet function. Frankly, we doubt that it is. Note that the principles of self-similarity described above carry over to the generalized forms as well.

The results of Eqs. (9) and (11) are in agreement with those of Kappraff and Adamson (2004), for which $b = 1$. In that case, we always have $\beta = -1/\alpha$. And of course, when $a = 1$, $\alpha = \varphi$.

Before showing some results for the generalized Binet formulae, we shall introduce some concepts from the literature on three-dimensional representations of the "other" Fibonacci spiral.

The Golden Shofar

Stakhov and Rozin (2004) have an interesting take on the Binet formula in the complex plane, as shown in Eq. (2). Here, we will point out a few highlights from their papers to set the stage for further exploration of the generalized Binet formulae. First, they identify the real and imaginary parts of Eq. (2) as follows

$$\begin{aligned} F(z) &= \frac{\varphi^x - \psi^x}{\varphi - \psi} = \frac{\varphi^x - (-1)^x \varphi^{-x}}{\sqrt{5}} \\ &= \frac{\varphi^x - \cos(\pi x)\varphi^{-x}}{\sqrt{5}} - i\frac{\sin(\pi x)\varphi^{-x}}{\sqrt{5}} \end{aligned} \tag{12}$$

Figure 5 shows a plot of the real part of $F(z)$. It is seen to be bound by two curves that Stakhov and Rozin term the symmetric hyperbolic Fibonacci functions, to wit,

$$\begin{aligned} cF(z) &= \frac{\varphi^x + \varphi^{-x}}{\sqrt{5}} = \frac{2}{\sqrt{5}}\cosh(x \ln \varphi) \\ sF(z) &= \frac{\varphi^x - \varphi^{-x}}{\sqrt{5}} = \frac{2}{\sqrt{5}}\sinh(x \ln \varphi) \end{aligned} \tag{13}$$

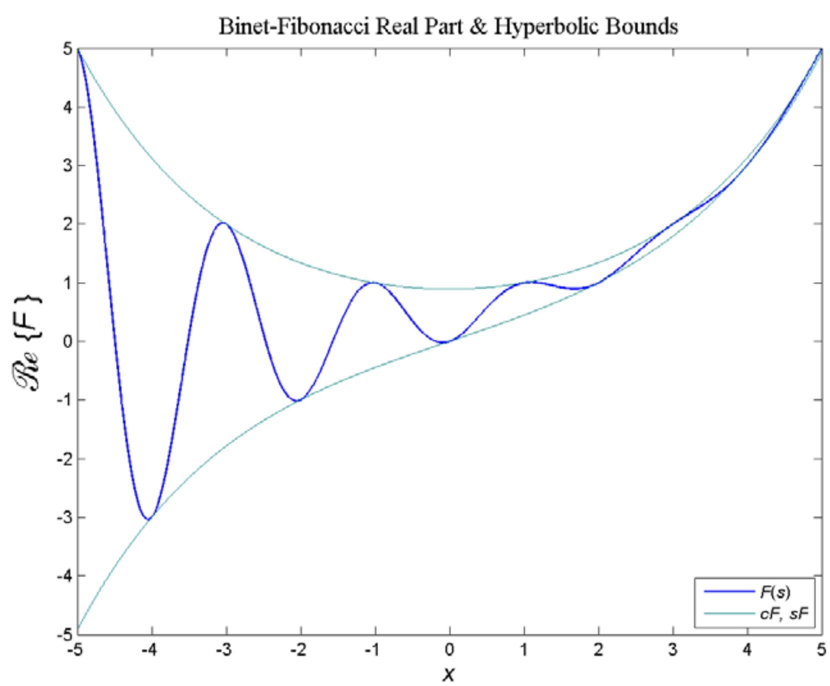

Figure 5: Real part of the Binet-Fibonacci formula and symmetric hyperbolic Fibonacci functions.

If we allow the imaginary of $F(z)$ to be in a perpendicular plane, then we can represent the "other" Fibonacci spiral as a three-dimensional curve in space. Figure 6 (left) shows that three-dimensional curve. This is the equivalent of taking Figure 1 and extruding the curves out normal to the page. When viewed in the Y-Z plane, we recover the 2-D spiral and curve as per Figure 1. Viewed in the X-Y plane, we have the real part of $F(z)$, as per Figure 5. Viewed in the X-Z plane we simply have the imaginary part of $F(z)$, a damped sinusoid.

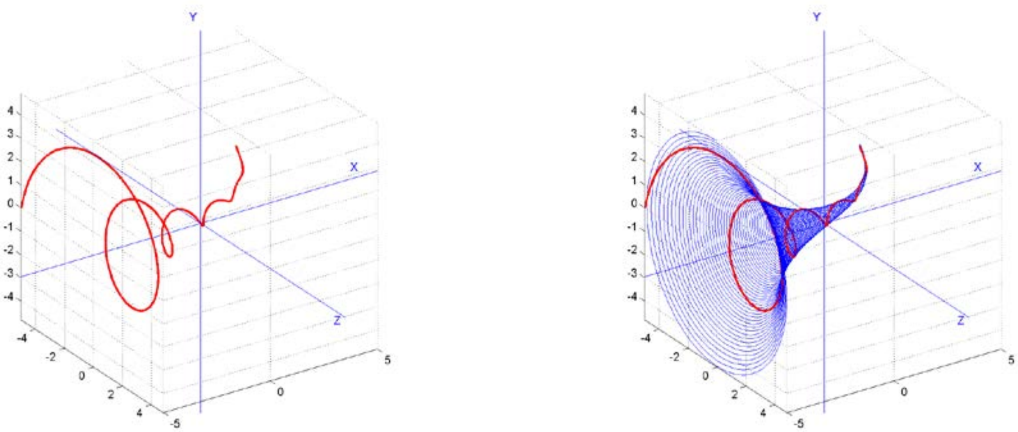

Figure 6: The three-dimensional "other" Fibonacci spiral (left) and bounding wire surface (right).

Now it gets really interesting. Stakhov and Rozin define a three-dimensional surface that is defined by this curve. It is shown in Figure 6 (right), where we have creating it by winding a wire about the midpoint of the hyperbolic curves at a radius equal to the local value of the imaginary part. This was also the basis of the accompanying animation. Stakhov and Rozin have dubbed this surface as the Golden Shofar. Translating from the Hebrew language, "Shofar" means horn, traditionally a ram or antelope horn; it is used ceremoniously on the Jewish New Year and Day of Atonement (Yom Kippur).

The surface is represented parametrically in standard Cartesian coordinates as

$$
\begin{aligned}
&c = \frac{cF + sF}{2} \\
&r = cF - c \\
&y(\theta) = r\cos\theta \\
&z(\theta) = r\sin\theta - c \\
&\theta \in [0, 2\pi]
\end{aligned}
\tag{14}
$$

Here, y is imaginary part of $F(z)$ and z is the real part. Figure 7 shows the full 3-D rendering of the surface, including front and back views of the surface itself, the bounding spiral (in red) and hyperbolic Fibonacci functions (in yellow). Figure 8 shows a comparison of the Fibonacci and Lucas shofars on the left and right, respectively. Taking a note from trumpet terminology, we can refer to the front and rear parts of the horn as the bell and mouthpiece, respectively.

Figure 7: 3-D surface model of the Golden Shofar; front (bell) and rear (mouthpiece) views.

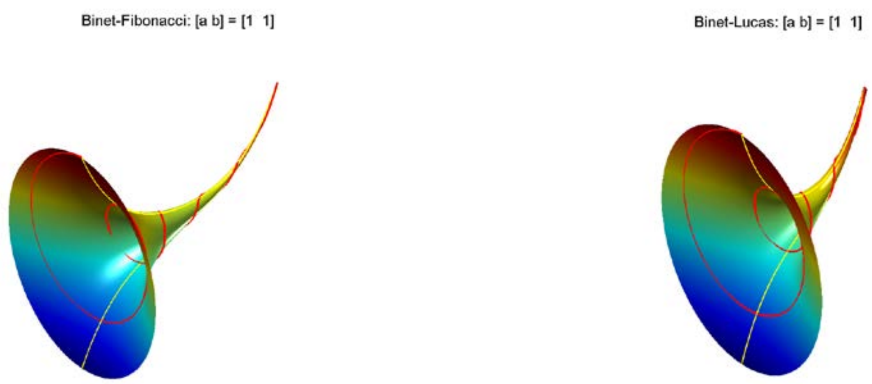

Figure 8: Comparison of the Fibonacci (left) and Lucas (right) shofars.

In the next section we will see the extent to which these ideas can be carried over the generalized Binet formulae.

Horn of plenty

Here, we will determine if the generalized Binet formulae will define shofar, or horn, surfaces for arbitrary values of the parameters *a* and *b*, as per Eq. (7). Specifically, we will see if the hyperbolic forms do indeed bound the real part of the real part of $F(z;a,b)$ and if the ensuing three-dimensional curves similarly define horn-shaped surfaces.

Without making a big deal of it, the answer to all these questions is, well, *yes*.

First, however, must define the (now) asymmetric hyperbolic Fibonacci and Lucas functions, i.e.,

	Fibonacci	Lucas
Cosine-type	$cF(z;a,b) = \dfrac{\alpha^x + \lvert\beta\rvert^x}{\alpha - \beta}$	$cL(z;a,b) = \alpha^x + \lvert\beta\rvert^x$
Sine-type	$sF(z;a,b) = \dfrac{\alpha^x - \lvert\beta\rvert^x}{\alpha - \beta}$	$sL(z;a,b) = \alpha^x - \lvert\beta\rvert^x$
$\alpha,\beta = \left(a \pm \sqrt{a^2+4b}\right)\big/2$		

These functions do indeed bound the real parts of $F(z;a,b)$ and $L(z;a,b)$. Recall that we mentioned earlier that when $b=1$ we have $\beta = -1/\alpha$. In that case, the asymmetric hyperbolic functions above devolve into the symmetric forms such as $\alpha^x \pm \alpha^{-x}$.

Second, the three-dimensional surfaces can be constructed in an exactly analogous way as described above. Several examples are shown in the Gallery (below) for random vales of *a* and *b*; they are given in the title on each figure. In some figures the position of the mouthpiece and bell are revered to provide a better view. And in many of the images the *x*-axis is stretched relative to the others because the spirals are otherwise too large to make out the shape if all axes are represented equally. However, before going there, some special cases are worth noting.

We have already noted that when $b=1$ we have symmetric hyperbolic functions. For integer values of *a*, say $a=n$, we have the well-known relations

$$\delta_n = \lim_{n\to\infty} \frac{F(z,n+1,1)}{F(z,n,1)} = \frac{n+\sqrt{n^2+4}}{2} \tag{15}$$

When $n=1$ we have Fibonacci sequence and this ratio is the golden ratio, i.e., $\delta_1 = \varphi$. When $n=2$ we have the Pell sequence, whose limit ratio, denoted $\delta_2 = 1+\sqrt{2}$, is called the silver ratio. And finally, when $n \geq 3$ (for which we do not think the sequences are named), the ratios are given by Eq. (15) and are called the bronze ratios, possibly denoted δ_n. In this report we shall simply use bronze ratio for $n = 3$, with a ratio of $\delta_3 = \left(3 + \sqrt{13}\right)/2$. These numbers are known collectively as the silver mean [Knott (2)]; they have the property that δ_n is n more than its reciprocal, i.e. $\delta_n = n + 1/\delta_n$. These have also been referred to as the metallic means: gold, silver, bronze, copper, nickel, … (unspecified) by de Spinadel (1999).

Figure 9 shows a comparison of the golden, silver, and bronze shofars, and a composite with all three. As *a* increases so the spirals grow faster.

Finally, we should remark that for large negative *x*-values, the *b* term dominates and the spirals devolve into logarithmic spirals and hence exhibit self-similarity.

Source code for generating the generalized Binet shofar surfaces is included in the Appendix.

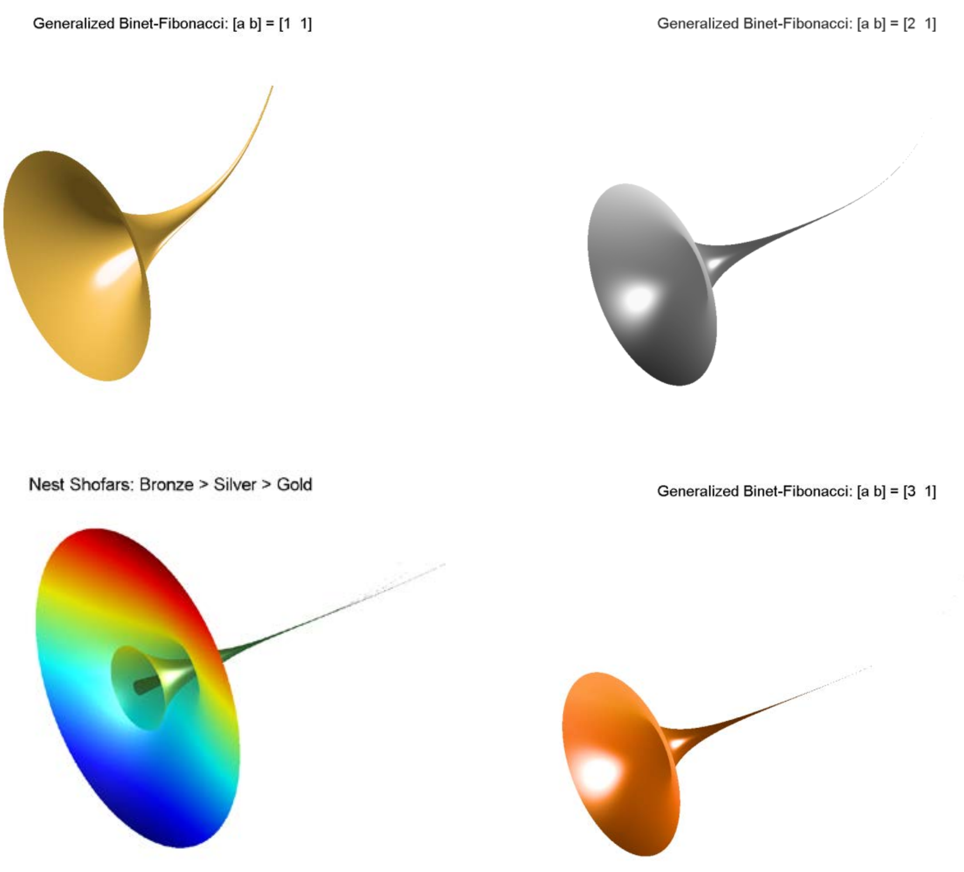

Figure 9: Comparison of the golden, silver, and bronze (indicated by color); in order of ascending magnitude.

Some comments on the Wiki page "Generalization of Fibonacci numbers"

In this Wikipedia entry (http://en.wikipedia.org/wiki/Generalizations_of_Fibonacci_numbers) extension of the Fibonacci numbers to all real and complex numbers is considered. The authors start with Binet's formula as we do, e.g.,

$$F(n) = \frac{\varphi^n - \psi^n}{\sqrt{5}} \tag{16}$$

Then choose the following functions (essentially the symmetric hyperbolic Fibonacci functions of Stakhov and Rozin) to represent the even and odd integers,

$$\begin{aligned} F_{even}(n) &= \frac{\varphi^n + \varphi^{-n}}{\sqrt{5}} \\ F_{odd}(n) &= \frac{\varphi^n - \varphi^{-n}}{\sqrt{5}} \end{aligned} \tag{17}$$

Or, alternatively,

$$F(x) = \frac{\varphi^x - \cos(\pi x)\varphi^{-x}}{\sqrt{5}} \tag{18}$$

They then claim that this equation can be solved for any real or complex value and that this is the complete generalized Fibonacci number of a complex variable.

This is an egregious error and serious misrepresentation of the extension of the Fibonacci number to the complex plane. Why? Because we have seen in Eq. (12) that Eq. (18) is only the real part of the complex Fibonacci number to begin with. The correct complex Fibonacci number was given previously as

$$F(z) = \frac{\varphi^x - \cos(\pi x)\varphi^{-x}}{\sqrt{5}} - i\frac{\sin(\pi x)\varphi^{-x}}{\sqrt{5}} \tag{19}$$

In other words, in seeking to find the complex Fibonacci number they have inadvertently discarded half of the problem. Simply put, one should say

$$\begin{gathered} F(z) = \frac{\varphi^z - (-1/\varphi)^z}{\sqrt{5}} = \frac{\varphi^z - (-1)^z \varphi^{-z}}{\sqrt{5}} \\ (-1)^z = e^{i\pi z} = \cos(\pi z) + i\sin(\pi z) \end{gathered} \tag{20}$$

And therein lies the problem. We see that they have discarded the imaginary part of $(-1)^z$ and it can never be recovered. Simply put, Eq. (18) is not the same as Eq. (16).

Summary and conclusions

We have demonstrated the "other" Fibonacci spiral and its three-dimensional curve and surface (the Golden Shofar). We have shown how these concepts can be carried through first to the derivatives of the Binet formula and then generalized Binet formulae of the Fibonacci- and Lucas-type. We have shown that the generalized Binet formulae with the fractional calculus and demonstrated differintegration with random complex orders. We have shown that Maynard's formula, which was developed for $a, b \in \mathbb{R}^+$, can be applied to some extent to negative values of *a* and *b*. In the simplest case, for $b = 1$, we have $F(z; -a, b) = -F(z; a, b)$.

This work presents many opportunities for further analysis.

References

de Bruijn, P.J. (1974). "An Extension of Fibonacci's Sequence," *The Fibonacci Quarterly*, **12**, 251-258.
http://www.fq.math.ca/Scanned/12-3/debruijn.pdf

Kappraff, J. and Adamson, G.W. (2004). "Generalized Binet Formulas, Lucas Polynomials, and Cyclic Constants," *Forma*, **19**, 355-366.
http://www.scipress.org/journals/forma/pdf/1904/19040355.pdf

Knott, R. (1) "Fibonacci Numbers and the Golden Section."
http://www.mcs.surrey.ac.uk/Personal/R.Knott/Fibonacci/

Knott, R. (2) "The Silver Means."
http://www.mcs.surrey.ac.uk/Personal/R.Knott/Fibonacci/cfINTRO.html#silver

Maynard, P. (2008). "Generalised Binet Formulas," *Applied Probability Trust*.
http://ms.appliedprobability.org/data/files/Articles%2040/40-3-2.pdf

Stakhov, A. and Rozin, B (2005). "The Golden Shofar," *Chaos, Solitons, and Fractals*, **26**, 677-684.
http://www.student.oulu.fi/~taneliha/Phi6/1/The%20Golden%20Shofar.pdf
See also http://www.mi.sanu.ac.rs/vismath/stakhov/

de Spinadel, V.W. (1999). "The Family of Metallic Means," *Visual Mathematics*, Vol. I, No. 3.
http://www.mi.sanu.ac.rs/vismath/spinadel/index.html

Waldman, C.H. (2013) "The Fibonacci Spiral and Pseudospirals," *National Curve Bank*
http://curvebank.calstatela.edu/waldman6/waldman6.htm

Gallery

Generalized Binet-Lucas: [a b] = [1.6667 1]

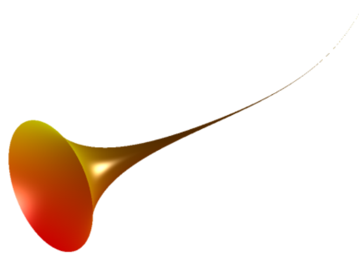

Generalized Binet-Fibonacci: [a b] = [0.5469 0.9575]

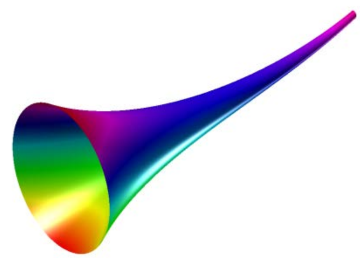

Generalized Binet-Lucas: [a b] = [0.034446 0.43874]

Generalized Binet-Lucas: [a b] = [-0.6431 0.70936]

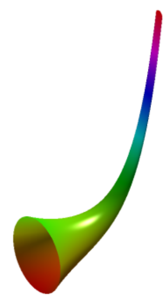

Generalized Binet-Lucas: [a b] = [0.81472 0.90579]

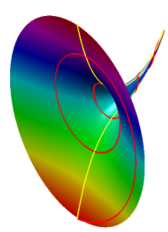

Binet-Fibonacci: [a b] = [0.33333 2.6667]

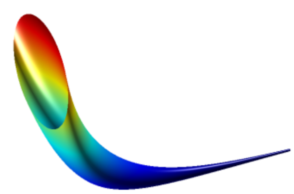

Generalized Binet-Fibonacci: [a b] = [-1.3905 0.8582]

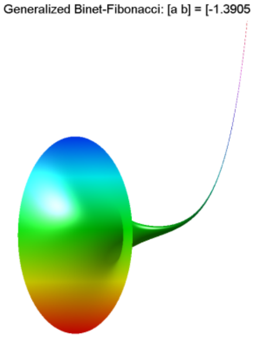

Generalized Binet-Lucas: [a b] = [1.5275 1.3384]

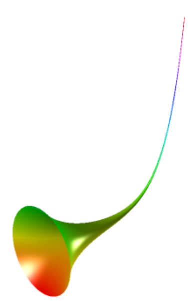

Appendix: Source code for Pseudospiral

```
function ShofarSurfaces

a=rand;          % b=1 with a=1,2,3 --> gold, silver, bronze shofars, resp
b=rand;
c=1;             % c=-1 --> Fibonacci-type, c=1 --> Lucas-type
plotcurve=1;     % 1 --> plot bounding curves, 0 --> don't

xpts=501;
xmax=5;
x=linspace(-xmax,xmax,xpts)';

[cfs,sfs]=HyperbolicGeneralBinet(x,a,b,c);
ctr=(cfs+sfs)/2;
r=(cfs-ctr)*0.99;

X=meshgrid(x);
t=linspace(0,2*pi,xpts);
[R,T]=meshgrid(r,t);
CTR=meshgrid(ctr);
Z=R.*sin(T)+CTR; % in physical space this should be y-coordinate
Y=R.*cos(T);     % in physical space this should be z-coordinate
figure
h=surf(X,Y,Z);
% consider -X when the bugle is backwards
set(h,'EdgeColor','none')
axis equal
axis off
colormap(hsv(1024))
material shiny
lighting gouraud
lightangle(80, -40)
lightangle(-90, 60)
if c==1
    title(['Generalized Binet-Lucas: [a b] = [' num2str([a b])
']'],'FontSize',14)
else
    title(['Generalized Binet-Fibonacci: [a b] = [' num2str([a b])
']'],'FontSize',14)
end

if plotcurve
    hold on
    z=GeneralBinetFn(x,a,b,c);
    plot3(x,imag(z),real(z),'r','LineWidth',2)
    Zs=zeros(size(x));
    plot3(x,Zs,cfs,'y','LineWidth',2)
    plot3(x,Zs,sfs,'y','LineWidth',2)
end

return
```

```
function y=GeneralBinetFn(n,a,b,c)
% generalized Binet function
% c=-1 is the Fibonacci function
% f(0)=0, f(1)=1, f(n+1)=a*f(n)+b*f(n-1) for n>=2
% c=-1 is the Lucas function
% f(0)=2, f(1)=a, f(n+1)=a*f(n)+b*f(n-1) for n>=2

alfa=(a+sqrt(a^2+4*b))/2;
beta=(a-sqrt(a^2+4*b))/2;

y=(alfa.^n+c*beta.^n);

if c==-1; y=y/(alfa+c*beta); end

return


function [chb,shb]=HyperbolicGeneralBinet(n,a,b,c)
% generalized hyperbolic Binet function
% c=-1 is the Fibonacci function
% f(0)=0, f(1)=1, f(n+1)=a*f(n)+b*f(n-1) for n>=2
% c=-1 is the Lucas function
% f(0)=2, f(1)=a, f(n+1)=a*f(n)+b*f(n-1) for n>=2

alfa=(a+sqrt(a^2+4*b))/2;
beta=(a-sqrt(a^2+4*b))/2;

chb=(alfa.^n+abs(beta).^n);
shb=(alfa.^n-abs(beta).^n);

if c==-1;
    chb=chb/(alfa+c*beta);
    shb=shb/(alfa+c*beta);
end

return
```